

Cosmological evolution of equation of state for dark energy in G-essence models

Kazuharu Bamba^{1,2,*}, Olga Razina², Koblandy Yerzhanov² and Ratbay Myrzakulov^{2,†}

¹*Kobayashi-Maskawa Institute for the Origin of Particles and the Universe,
Nagoya University, Nagoya 464-8602, Japan*

²*Eurasian International Center for Theoretical Physics, Dep. Gen. & Theor.
Phys., Eurasian National University, Astana 010008, Kazakhstan*

Abstract

We explore the cosmological evolution of equation of state (EoS) for dark energy in g-essence models, the action of which is described by a function of both the canonical kinetic term of both the scalar and fermionic fields. We examine g-essence models with realizing the crossing of the phantom divide line of $w_{\text{DE}} = -1$ as well as the models in which the universe always stays in the non-phantom (quintessence) phase ($w_{\text{DE}} > -1$). In particular, we find an explicit g-essence model with the crossing from the non-phantom phase to the phantom one ($w_{\text{DE}} < -1$). This transition behavior is consistent with the recent observational data analyses.

PACS numbers: 95.36.+x, 98.80.-k

* E-mail address: bamba@kmi.nagoya-u.ac.jp

† E-mail addresses: rmyrzakulov@gmail.com

I. INTRODUCTION

According to recent cosmological observations such as Type Ia Supernovae [1, 2], cosmic microwave background (CMB) radiation [3–7], large scale structure (LSS) [8, 9], baryon acoustic oscillations (BAO) [10], and weak lensing [11], the expansion of the current universe is accelerating.

There are two categories to explain the current cosmic acceleration. One is to suppose the existence of some unknown matters called dark energy. The other is to modify gravity. There are a number of candidates for dark energy, e.g., the cosmological constant, scalar fields like quintessence [12–16] and k-essence [17–22], and fluid as a Chaplygin gas [23, 24] (for reviews, see, e.g., [25–32], and for related works, see, for example, [33–37]). There also exist several ways of modification of gravity, e.g., $F(R)$ gravity (for recent reviews, see, e.g., [38–45]).

One of the most important quantities in the studies in terms of the property of dark energy is the equation of state (EoS). It seem to be suggested by recent various cosmological and astronomical observational data [46–51] that the crossing of the phantom divide line of $w_{\text{DE}} = -1$ occurred in the near past, where w_{DE} is the EoS for dark energy. There are a lot of theoretical attempts and proposals to account for such a phantom crossing phenomenon in the framework of both dark energy in general relativity and modified gravity scenarios in the literature (for references, see, e.g., the review articles shown above [25–31, 38–44].).

In addition, on the theoretical studies, as phenomenological generalizations of k-essence models, the action of which is written by a function of the canonical kinetic term of a scalar field, f-essence and g-essence models have recently been proposed in Ref. [52]. The action of f-essence is described by a function of the canonical kinetic term of a fermionic field. On the other hand, the action of g-essence is represented by a function of the canonical kinetic term of a scalar field as well as that of a fermionic field, which corresponds to a generalized theory constructed by combining k-essence with f-essence. In this paper, we concentrate on the evolutions of cosmological quantities, especially the EoS for dark energy in g-essence models. We analyze the evolutions of cosmological quantities in g-essence models with realizing the crossing of the phantom divide as well as without it. In particular, we examine g-essence models in which the universe always evolves within the non-phantom (quintessence) phase ($w_{\text{DE}} > -1$). In addition, we find an explicit g-essence model with

realizing the crossing of the phantom divide line of $w_{\text{DE}} = -1$ from the non-phantom phase to the phantom one ($w_{\text{DE}} < -1$). It is interesting to emphasize that this transition behavior is compatible with the data analyses of the recent cosmological observations [46–51]. It has also been investigated that in viable $f(R)$ gravity models, the phantom crossing with the opposite manner (i.e., from the phantom phase to the non-phantom phantom one) can occur (see, e.g., [53] and the references therein), whereas in $f(T)$ theories, where T is the torsion scalar, the phantom crossing with the same transition direction (i.e., from the non-phantom phase to the phantom one) can happen [54–56] (for related aspects in $f(T)$ theories, see, e.g., [57–59]).

The most significant physical motivation of this work is to illustrate the cosmological evolution of the EoS for dark energy w_{DE} in g-essence models. This is inspired by the data analysis of recent cosmological and astronomical observations [46–51], which implies that the crossing of the phantom divide happened in the near past. On the other hand, it is known that in the so-called “reconstruction” [60–69], we starts with a well motivated theoretical model such as simplicity and/or analogy with some fundamental theory, and by using its form derives an expansion law of the universe to be compared with observational data, or inversely, starts with the observational data themselves and try to fit them with a theoretical model. Our demonstrations in this work are complementary to such reconstruction processes.

The paper is organized as follows. In Sec. II, we briefly explain g-essence, k-essence and f-essence models. In Sec. III, we investigate a particular g-essence model and the evolutions of cosmological quantities. In Sec. IV, we explore g-essence models both with and without the crossing of the phantom divide. Finally, conclusions are presented in Sec. V.

II. ESSENCE MODELS

In this section, we explain g-essence, k-essence and f-essence models.

A. g-essence

The action of g-essence is given by [52]

$$S = \int d^4x \sqrt{-g} [R + 2K(X, Y, \phi, \psi, \bar{\psi})], \quad (2.1)$$

where K is some function of its arguments, ϕ is a scalar function, $\psi = (\psi_1, \psi_2, \psi_3, \psi_4)^T$ is a fermionic function and $\bar{\psi} = \psi^\dagger \gamma^0$ is its adjoint function. Here, the canonical kinetic term for the scalar field X and fermionic field Y are given by

$$X = 0.5g^{\mu\nu}\nabla_\mu\phi\nabla_\nu\phi, \quad Y = 0.5i[\bar{\psi}\Gamma^\mu D_\mu\psi - (D_\mu\bar{\psi})\Gamma^\mu\psi], \quad (2.2)$$

where ∇_μ and D_μ are the covariant derivatives. We note that here the fermionic fields are treated as classically commuting fields.

We consider the flat Friedmann-Lemaître-Robertson-Walker (FLRW) space-time with the metric,

$$ds^2 = dt^2 - a^2(dx^2 + dy^2 + dz^2), \quad (2.3)$$

where $a(t)$ is the scale factor, and the vierbein is chosen to be (see, e.g., [70])

$$(e_a^\mu) = \text{diag}(1, 1/a, 1/a, 1/a), \quad (e_a^\alpha) = \text{diag}(1, a, a, a). \quad (2.4)$$

In the case of the flat FLRW metric (2.3), from the action (2.1) the basic equations read [52]

$$3H^2 - \rho = 0, \quad (2.5)$$

$$2\dot{H} + 3H^2 + p = 0, \quad (2.6)$$

$$K_X\ddot{\phi} + (\dot{K}_X + 3HK_X)\dot{\phi} - K_\phi = 0, \quad (2.7)$$

$$K_Y\dot{\psi} + 0.5(3HK_Y + \dot{K}_Y)\psi - i\gamma^0 K_{\bar{\psi}} = 0, \quad (2.8)$$

$$K_Y\dot{\bar{\psi}} + 0.5(3HK_Y + \dot{K}_Y)\bar{\psi} + iK_\psi\gamma^0 = 0, \quad (2.9)$$

$$\dot{\rho} + 3H(\rho + p) = 0, \quad (2.10)$$

where the kinetic terms, the energy density and pressure take the forms

$$X = 0.5\dot{\phi}^2, \quad Y = 0.5i(\bar{\psi}\gamma^0\dot{\psi} - \dot{\bar{\psi}}\gamma^0\psi), \quad \rho = 2K_X X + K_Y Y - K, \quad p = K. \quad (2.11)$$

Here, a dot denotes a time derivative of $\partial/\partial t$ and $H = \dot{a}/a$ is the Hubble parameter. Moreover, the subscription of K , e.g., $K_X \equiv \partial K/\partial X$, denotes the derivative of K with respect to X . Several properties of g -essence have been studied in Refs. [71–74]. We remark that the model (2.1) can also describe *k-essence* and *f-essence*, as is shown in the following next subsections.

B. k-essence

We examine the case that the Lagrangian K has the form

$$K = K_1 = K_1(X, \phi). \quad (2.12)$$

Then, the action (2.1) takes the form [52]

$$S = \int d^4x \sqrt{-g} [R + 2K_1(X, \phi)], \quad (2.13)$$

which corresponds to k-essence [17–22] (for a solvable case, see [75]). For the flat FLRW metric (2.3), the basic equations of k-essence becomes [17–22]

$$3H^2 - \rho = 0, \quad (2.14)$$

$$2\dot{H} + 3H^2 + p = 0, \quad (2.15)$$

$$K_X \ddot{\phi} + (\dot{K}_X + 3HK_X)\dot{\phi} - K_\phi = 0, \quad (2.16)$$

$$\dot{\rho} + 3H(\rho + p) = 0. \quad (2.17)$$

C. f-essence

Now, we consider the case that the Lagrangian K takes the form

$$K = K_2 = K_2(Y, \psi, \bar{\psi}). \quad (2.18)$$

In this case, the action (2.1) is written as

$$S = \int d^4x \sqrt{-g} [R + 2K_2(Y, \psi, \bar{\psi})]. \quad (2.19)$$

This is the so-called f-essence [52]. In the case of the flat FLRW metric (2.3), the basic equations in f-essence have the forms [52]

$$3H^2 - \rho = 0, \quad (2.20)$$

$$2\dot{H} + 3H^2 + p = 0, \quad (2.21)$$

$$K_Y \dot{\psi} + 0.5(3HK_Y + \dot{K}_Y)\psi - i\gamma^0 K_{\bar{\psi}} = 0, \quad (2.22)$$

$$K_Y \dot{\bar{\psi}} + 0.5(3HK_Y + \dot{K}_Y)\bar{\psi} + iK_\psi \gamma^0 = 0, \quad (2.23)$$

$$\dot{\rho} + 3H(\rho + p) = 0, \quad (2.24)$$

where the energy density and pressure are expressed as

$$\rho = K_Y Y - K, \quad p = K. \quad (2.25)$$

It is important to note that in addition to the description of a spinor field of f-essence as a classical c-number quantity, it can also be treated as a Grassmann-valued quantity (see, e.g., [76]), or as an operator (“q-number”), as in Ref. [77].

III. PARTICULAR G-ESSENCE MODEL

In general, in g-essence models [52] equations of motion are very complicated and therefore it is difficult to obtain those exact analytical solutions. In contrast to such more general and complex cases, in order to execute the analyses we here explore the following more simple particular model

$$K = \epsilon X + \sigma Y - V_1(\phi) - V_2(u), \quad (3.1)$$

where $u = \bar{\psi}\psi$, and ϵ and σ are constants. In this model, the equation system (2.9)–(2.14) is described as

$$3H^2 - \rho = 0, \quad (3.2)$$

$$2\dot{H} + 3H^2 + p = 0, \quad (3.3)$$

$$\epsilon\ddot{\phi} + 3\epsilon H\dot{\phi} + V_{1\phi} = 0, \quad (3.4)$$

$$\sigma\dot{\psi} + \frac{3}{2}\sigma H\psi + iV_2'\gamma^0\psi = 0, \quad (3.5)$$

$$\sigma\dot{\bar{\psi}} + \frac{3}{2}\sigma H\bar{\psi} - iV_2'\bar{\psi}\gamma^0 = 0, \quad (3.6)$$

$$\dot{\rho} + 3H(\rho + p) = 0, \quad (3.7)$$

where

$$\rho = 0.5\epsilon\dot{\phi}^2 + V_1 + V_2, \quad (3.8)$$

$$p = 0.5\epsilon\dot{\phi}^2 - V_1 - V_2 + V_2'u. \quad (3.9)$$

Here, a prime denotes the derivative of a quantity with respect of its argument such as $V' \equiv \partial V/\partial u$. We note that the contribution of the fermion field is included in the potential $V_2(u)$.

IV. COSMOLOGICAL SOLUTIONS

In this section, we analyze cosmological solutions in several examples with $V_1 = 0$ in the particular g-essence model shown in Sec. III. In particular, we examine the cosmological evolutions of the energy density ρ and pressure p , the deceleration parameter $q \equiv -\ddot{a}/(aH^2)$, the jerk parameter $j \equiv \ddot{a}'/(aH^3)$ [78], and the EoS $w \equiv p/\rho$ as functions of t . We study both four examples with and those without the crossing of the phantom divide. We note that the subscription $i = 1, 2, \dots, 8$ of ρ_i, p_i, q_i, j_i and w_i denotes the number of four examples in Secs. IV A 1–4 ($i = 1, 2, 3, 4$) and those in IV B 1–4 ($i = 5, 6, 7, 8$). In the Λ Cold Dark Matter (CDM) model, $q = -1$, $j = 1$ and $w = -1$, and hence these quantities denote the deviation of a model from the Λ CDM model. In what follows, we consider the dark energy dominated stage in which dark energy (which is, e.g., g-essence in this paper) is dominant over the universe, and therefore it can be interpreted that $w \approx w_{\text{DE}}$, where w_{DE} is the EoS for dark energy.

It is known that in the FLRW background (2.3), the effective EoS for the universe is given by [38, 39] $w_{\text{eff}} \equiv p_{\text{eff}}/\rho_{\text{eff}} = -1 - 2\dot{H}/(3H^2)$ with $\rho_{\text{eff}} \equiv 3H^2/\kappa^2$ and $p_{\text{eff}} \equiv -(2\dot{H} + 3H^2)/\kappa^2$ being the effective energy density and pressure of the universe. Here, ρ_{eff} and p_{eff} correspond to the total energy density and pressure of the universe, respectively. If the energy density of dark energy is dominant over that of matter completely, $w_{\text{DE}} \approx w_{\text{eff}}$. In the non-phantom (quintessence) phase, $\dot{H} < 0$ and hence $w_{\text{eff}} > -1$, whereas in the phantom phase, $\dot{H} > 0$ and therefore $w_{\text{eff}} < -1$. Moreover, for $\dot{H} = 0$, $w_{\text{eff}} = -1$, which corresponds to the cosmological constant. From the above considerations, we examine the case that $w \approx w_{\text{DE}} \approx w_{\text{eff}}$.

In case of $V_1 = 0$, the system (3.2)–(3.7) becomes

$$3H^2 - \rho = 0, \quad (4.1)$$

$$2\dot{H} + 3H^2 + p = 0, \quad (4.2)$$

$$\ddot{\phi} + 3H\dot{\phi} = 0, \quad (4.3)$$

$$\sigma\dot{\psi} + \frac{3}{2}\sigma H\psi + iV_2'\gamma^0\psi = 0, \quad (4.4)$$

$$\sigma\dot{\bar{\psi}} + \frac{3}{2}\sigma H\bar{\psi} - iV_2'\bar{\psi}\gamma^0 = 0, \quad (4.5)$$

$$\dot{\rho} + 3H(\rho + p) = 0, \quad (4.6)$$

where

$$\rho = 0.5\epsilon\dot{\phi}^2 + V_2, \quad (4.7)$$

$$p = 0.5\epsilon\dot{\phi}^2 - V_2 + V_2' u. \quad (4.8)$$

As a result, we find

$$u = \frac{c}{a^3}, \quad \dot{\phi} = \frac{\phi_0}{a^3}, \quad V_2 = -\frac{0.5\epsilon\phi_0^2}{a^6} + 3H^2, \quad (4.9)$$

and

$$\psi_l = \frac{c_l}{a^{1.5}} e^{iD}, \quad \psi_k = \frac{c_k}{a^{1.5}} e^{-iD}, \quad (4.10)$$

where c and ϕ_0 are constants. Here, $l = 0, 1$, $k = 2, 3$, c_j ($j = 0, \dots, 3$) obey the following condition $c = |c_0|^2 + |c_1|^2 - |c_2|^2 - |c_3|^2$, and

$$D = \frac{1}{c \sigma} \left(2 \int a^3 dH + \phi_0^2 \int a^{-3} dt \right). \quad (4.11)$$

A. Solutions without the crossing of the phantom divide

In this subsection, we explore derive the solutions in four examples without the crossing of the phantom divide.

1. Example 1

We start from the following expression for the scale factor

$$a = e^{\frac{2}{3} \int \frac{dt}{t - 0.5(t^2 \sin[\frac{1}{t}] + t \cos[\frac{1}{t}] + Si[\frac{1}{t}])}}, \quad (4.12)$$

where

$$Si[x] = \int_0^x \frac{\sin[z]}{z} dz. \quad (4.13)$$

In this case, we obtain

$$H = \frac{2}{3[t - 0.5(t^2 \sin[\frac{1}{t}] + t \cos[\frac{1}{t}] + Si[\frac{1}{t}])]}, \quad (4.14)$$

$$u = c e^{-2 \int \frac{dt}{t - 0.5(t^2 \sin[\frac{1}{t}] + t \cos[\frac{1}{t}] + Si[\frac{1}{t}])}}, \quad (4.15)$$

$$\dot{\phi} = \phi_0 e^{-2 \int \frac{dt}{t - 0.5(t^2 \sin[\frac{1}{t}] + t \cos[\frac{1}{t}] + Si[\frac{1}{t}])}}, \quad (4.16)$$

$$\psi_l = c_l e^{iD - \int \frac{dt}{t - 0.5(t^2 \sin[\frac{1}{t}] + t \cos[\frac{1}{t}] + Si[\frac{1}{t}])}}, \quad (4.17)$$

$$\psi_k = c_k e^{-iD - \int \frac{dt}{t - 0.5(t^2 \sin[\frac{1}{t}] + t \cos[\frac{1}{t}] + Si[\frac{1}{t}])}}, \quad (4.18)$$

where

$$D = \frac{1}{c \sigma} \int \left[\frac{4(1 - t \sin[\frac{1}{t}])}{3[t - 0.5(t^2 \sin[\frac{1}{t}] + t \cos[\frac{1}{t}] + Si[\frac{1}{t}])]^2} e^{2 \int \frac{dt}{t - 0.5(t^2 \sin[\frac{1}{t}] + t \cos[\frac{1}{t}] + Si[\frac{1}{t}])}} + \phi_0^2 e^{-2 \int \frac{dt}{t - 0.5(t^2 \sin[\frac{1}{t}] + t \cos[\frac{1}{t}] + Si[\frac{1}{t}])}} \right] dt. \quad (4.19)$$

The corresponding potential has the form

$$V_2 = -0.5 \epsilon \phi_0^2 e^{-4 \int \frac{dt}{t - 0.5(t^2 \sin[\frac{1}{t}] + t \cos[\frac{1}{t}] + Si[\frac{1}{t}])}} + \frac{4}{3[t - 0.5(t^2 \sin[\frac{1}{t}] + t \cos[\frac{1}{t}] + Si[\frac{1}{t}])]^2}. \quad (4.20)$$

The energy density and pressure are described by

$$\rho_1 = \frac{4}{3[t - 0.5(t^2 \sin[\frac{1}{t}] + t \cos[\frac{1}{t}] + Si[\frac{1}{t}])]^2},$$

$$p_1 = -\frac{4t \sin \frac{1}{t}}{3[t - 0.5(t^2 \sin[\frac{1}{t}] + t \cos[\frac{1}{t}] + Si[\frac{1}{t}])]^2}. \quad (4.21)$$

For this example, the EoS and the deceleration parameter have the form

$$w_1 \equiv \frac{p_1}{\rho_1} = -t \sin[\frac{1}{t}], \quad (4.22)$$

and

$$q_1 \equiv -\frac{\ddot{a}}{aH^2} = 0.5 - 1.5t \sin[\frac{1}{t}]. \quad (4.23)$$

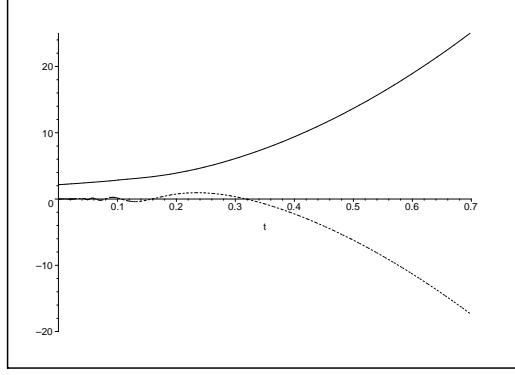


FIG. 1: ρ_1 (solid line) and p_1 (dotted line) as a functions of t .

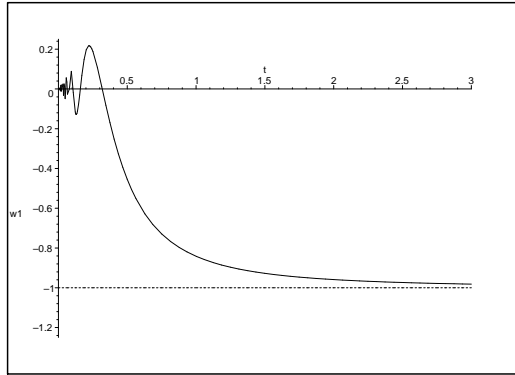


FIG. 2: w_1 as a function of t .

In Fig. 1, we show the cosmological evolutions of the energy density ρ_1 and pressure p_1 as the functions of t . Furthermore, in Fig. 2 we depict the cosmological evolutions of the EoS w_1 as a function of t . From Fig. 2 we see that in this model the crossing of the phantom divide cannot be realized. In addition, the jerk parameter is defined as

$$\begin{aligned}
 j_1 &\equiv \frac{\ddot{a}}{aH^3} = \frac{\ddot{a}a^2}{\dot{a}^3} \\
 &= 1 - \frac{9}{8t} \left[(2 - 3t^3) \sin^2\left[\frac{1}{t}\right] + Si\left[\frac{1}{t}\right] \left(t \sin\left[\frac{1}{t}\right] - \cos\left[\frac{1}{t}\right] \right) + t \cos\left[\frac{1}{t}\right] \left(2 - \cos\left[\frac{1}{t}\right] \right) \right]. \quad (4.24)
 \end{aligned}$$

In Fig. 3, we plot the deceleration parameter q_1 and jerk parameter j_1 as functions of t .

2. Example 2

We suppose that the scale factor is described by the following expression

$$a = e^{\frac{2}{3} \int \frac{dt}{t - e^{0.5t-1}(t+1)^{0.5(t^2-1)}t^{-0.5t^2}}}. \quad (4.25)$$

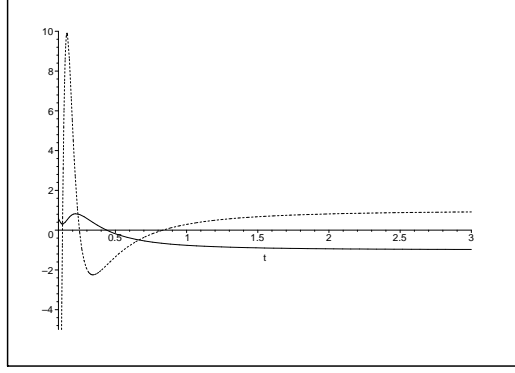


FIG. 3: q_1 (solid line) and j_1 (dotted line) as functions of t .

Then, we find

$$H = \frac{2}{3[t - e^{0.5t-1}(t+1)^{0.5(t^2-1)}t^{-0.5t^2}]}, \quad (4.26)$$

$$u = c e^{-2 \int \frac{dt}{t - e^{0.5t-1}(t+1)^{0.5(t^2-1)}t^{-0.5t^2}}}, \quad (4.27)$$

$$\dot{\phi} = \phi_0 e^{-2 \int \frac{dt}{t - e^{0.5t-1}(t+1)^{0.5(t^2-1)}t^{-0.5t^2}}}, \quad (4.28)$$

$$\psi_l = c_l e^{iD \int \frac{dt}{t - e^{0.5t-1}(t+1)^{0.5(t^2-1)}t^{-0.5t^2}}}, \quad (4.29)$$

$$\psi_k = c_k e^{-iD \int \frac{dt}{t - e^{0.5t-1}(t+1)^{0.5(t^2-1)}t^{-0.5t^2}}}, \quad (4.30)$$

where

$$D = \frac{1}{c \sigma} \int \left[\frac{4(-t-1 + e^{0.5t-1}(t+1)^{0.5(t^2+1)}t^{-0.5t^2} \ln \frac{t+1}{t})}{3(t\sqrt{t+1} - e^{0.5t-1}(t+1)^{0.5t^2}t^{-0.5t^2})} \right. \\ \left. \times e^{2 \int \frac{dt}{t - e^{0.5t-1}(t+1)^{0.5(t^2-1)}t^{-0.5t^2}}} + \phi_0^2 \int e^{-2 \int \frac{dt}{t - e^{0.5t-1}(t+1)^{0.5(t^2-1)}t^{-0.5t^2}}} \right] dt. \quad (4.31)$$

The form of the corresponding potential is given by

$$V_2 = -0.5\epsilon\phi_0^2 e^{-4 \int \frac{dt}{t - e^{0.5t-1}(t+1)^{0.5(t^2-1)}t^{-0.5t^2}}} + \frac{4}{3[t - e^{0.5t-1}(t+1)^{0.5(t^2-1)}t^{-0.5t^2}]^2}. \quad (4.32)$$

The energy density and pressure are expressed as

$$\rho_2 = \frac{4}{3(t - e^{0.5t-1}(t+1)^{0.5(t^2-1)}t^{-0.5t^2})^2}, \quad p_2 = -\frac{4(1 + \frac{1}{t})^t}{3e(t - e^{0.5t-1}(t+1)^{0.5(t^2-1)}t^{-0.5t^2})^2}. \quad (4.33)$$

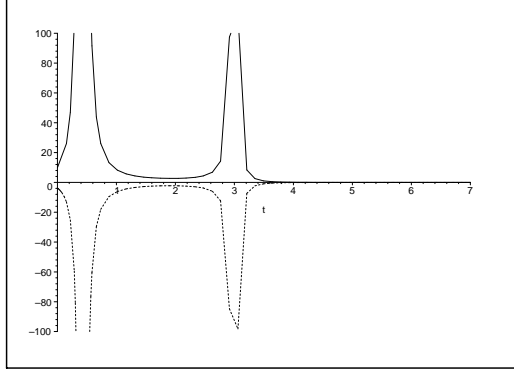


FIG. 4: ρ_2 (solid line) and p_2 (dotted line) as functions of t .

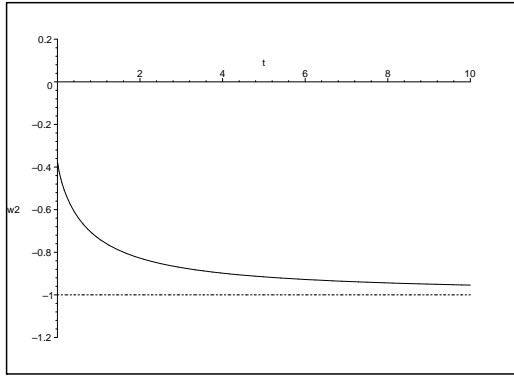


FIG. 5: w_2 as a function of t .

In case of this example, the EoS and the deceleration parameter become

$$w_2 = -e^{-1}\left(1 + \frac{1}{t}\right)^t, \quad (4.34)$$

and

$$q_2 = 0.5 - 1.5e^{-1}\left(1 + \frac{1}{t}\right)^t. \quad (4.35)$$

In Fig. 4, we illustrate the cosmological evolutions of the energy density ρ_2 and pressure p_2 as functions of t . In Fig. 5, we show the cosmological evolutions of the EoS w_2 as a function of t . It follows from Fig. 5 that the crossing of the phantom divide cannot occur in this example. In Fig. 6, we plot the deceleration parameter q_2 and jerk parameter j_2^1 as functions of t .

¹ In Fig. 6, we have plotted the behavior of j_2 numerically because the analytic expression is too complicated. This is the same as for j_3 in Fig. 10 in Sec. IV A 3.

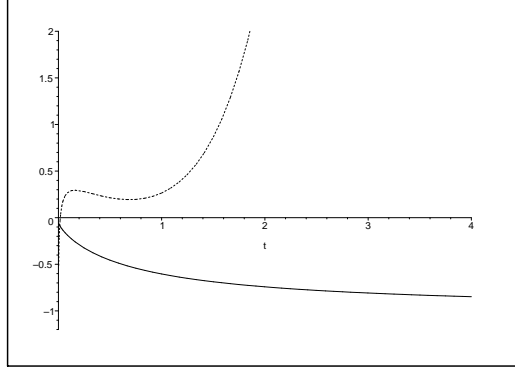


FIG. 6: q_2 (solid line) and j_2 (dotted line) as functions of t .

3. Example 3

We provide that the scale factor is expressed as

$$a = e^{\frac{2}{3} \int \frac{dt}{t - A^{0.5A^2} e^{A(0.5t-1)} (t+A)^{0.5(t^2-A^2)} t^{-0.5t^2}}, \quad (4.36)$$

where A is a constant. From this expression, we have

$$H = \frac{2}{3[t - A^{0.5A^2} e^{A(0.5t-1)} (t+A)^{0.5(t^2-A^2)} t^{-0.5t^2}]}, \quad (4.37)$$

$$u = c e^{-2 \int \frac{dt}{t - A^{0.5A^2} e^{A(0.5t-1)} (t+A)^{0.5(t^2-A^2)} t^{-0.5t^2}}, \quad (4.38)$$

$$\dot{\phi} = \phi_0 e^{-2 \int \frac{dt}{t - A^{0.5A^2} e^{A(0.5t-1)} (t+A)^{0.5(t^2-A^2)} t^{-0.5t^2}}, \quad (4.39)$$

$$\psi_l = c_l e^{iD \int \frac{dt}{t - A^{0.5A^2} e^{A(0.5t-1)} (t+A)^{0.5(t^2-A^2)} t^{-0.5t^2}}, \quad (4.40)$$

$$\psi_k = c_k e^{-iD \int \frac{dt}{t - A^{0.5A^2} e^{A(0.5t-1)} (t+A)^{0.5(t^2-A^2)} t^{-0.5t^2}}, \quad (4.41)$$

where

$$D = \frac{1}{c \sigma} \int \left[\frac{4(-1 + A^{0.5A^2} e^{A(0.5t-1)} (t+A)^{0.5(t^2-A^2)} t^{-0.5t^2+1} \ln \frac{t+A}{t})}{3(t - A^{0.5A^2} e^{A(0.5t-1)} (t+A)^{0.5(t^2-A^2)} t^{-0.5t^2})^2} \times \right. \\ \times e^{2 \int \frac{dt}{t - A^{0.5A^2} e^{A(0.5t-1)} (t+A)^{0.5(t^2-A^2)} t^{-0.5t^2}} + \\ \left. + \phi_0^2 e^{-2 \int \frac{dt}{t - A^{0.5A^2} e^{A(0.5t-1)} (t+A)^{0.5(t^2-A^2)} t^{-0.5t^2}} \right] dt. \quad (4.42)$$

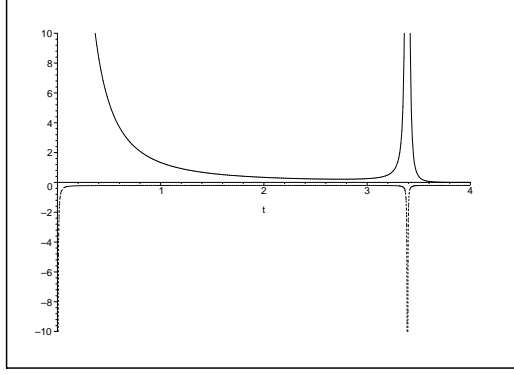


FIG. 7: ρ_3 (solid line) and p_3 (dotted line) as functions of t for $A = 10$.

The corresponding potential becomes

$$V_2 = -0.5\epsilon\phi_0^2 e^{-4 \int \frac{dt}{t - A^{0.5A^2} e^{A(0.5t-1)} (t+A)^{0.5(t^2-A^2)} t^{-0.5t^2}} + \frac{4}{3[t - A^{0.5A^2} e^{A(0.5t-1)} (t+A)^{0.5(t^2-A^2)} t^{-0.5t^2}]^2}. \quad (4.43)$$

The energy density and pressure are given by

$$\rho_3 = \frac{4}{3[t - A^{0.5A^2} e^{A(0.5t-1)} (t+A)^{0.5(t^2-A^2)} t^{-0.5t^2}]^2}, \quad (4.44)$$

$$p_3 = -\frac{4(1 + \frac{A}{t})^t}{3e^A [t - A^{0.5A^2} e^{A(0.5t-1)} (t+A)^{0.5(t^2-A^2)} t^{-0.5t^2}]^2}. \quad (4.45)$$

In this example, the EoS and the deceleration parameter are written as

$$w_3 = -e^{-A} \left(1 + \frac{A}{t}\right)^t \quad (4.46)$$

and

$$q_3 = 0.5 - 1.5e^{-A} \left(1 + \frac{A}{t}\right)^t, \quad (4.47)$$

respectively.

In Fig. 7, we plot the cosmological evolutions of the energy density ρ_3 and pressure p_3 as functions of t for $A = 10$. In Fig. 8, we display the cosmological evolution of the EoS w_3 as a function of t for $A = 10$. We find from Fig. 8 that in this model the crossing of the phantom divide cannot happen. In Fig. 9, we show the cosmological evolution of the deceleration parameter q_3 as a function of t . In Fig. 10, we illustrate the cosmological evolution of the jerk parameter j_3^2 as a function of t .

² See the footnote in Sec. IV A 2.

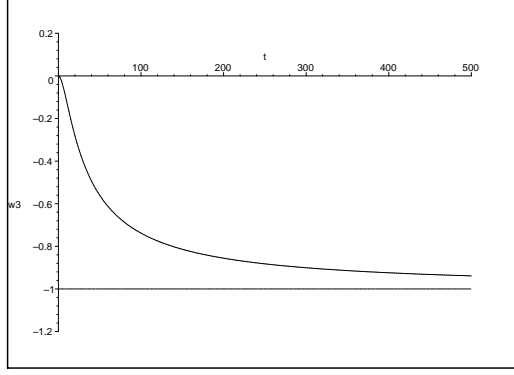


FIG. 8: w_3 as a function of t for $A = 10$.

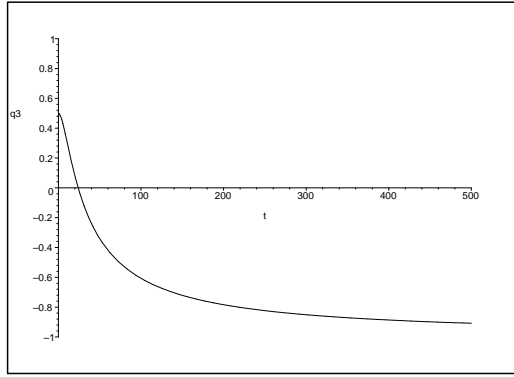


FIG. 9: q_3 (solid line) as a function of t .

4. Example 4

We consider that the scale factor is written by

$$a = (a_0 + b \cosh[kt] + d \sinh[kt])^{\frac{1}{3}}, \quad (4.48)$$

where a_0 , b , d and k are constants. In this case, we acquire

$$H = \frac{k(b \sinh[kt] + d \cosh[kt])}{3(a_0 + b \cosh[kt] + d \sinh[kt])^{\frac{2}{3}}}, \quad (4.49)$$

$$u = \frac{c}{a_0 + b \cosh[kt] + d \sinh[kt]}, \quad (4.50)$$

$$\phi = \frac{2\phi_0^2}{k\sqrt{b^2 - d^2 - a_0^2}} \arctan\left(\frac{(b - a_0) \tanh[0.5kt] + d}{\sqrt{b^2 - d^2 - a_0^2}}\right), \quad (4.51)$$

$$\psi_l = \frac{c_l}{(a_0 + b \cosh[kt] + d \sinh[kt])^2} e^{iD}, \quad (4.52)$$

$$\psi_k = \frac{c_k}{(a_0 + b \cosh[kt] + d \sinh[kt])^2} e^{-iD}, \quad (4.53)$$

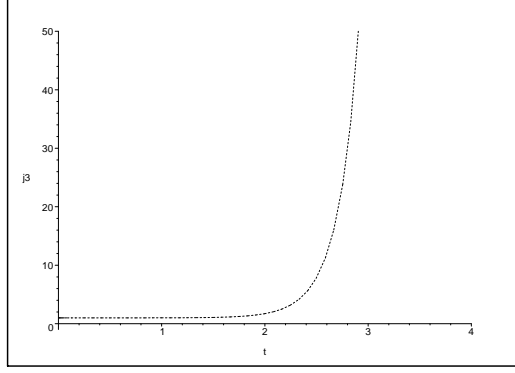


FIG. 10: j_3 (dotted line) as a function of t .

where

$$D = \frac{2k}{3c\sigma} \left[\frac{2(b^2 - d^2 - a_0^2 + \frac{3\phi_0^2}{2k^2})}{\sqrt{b^2 - d^2 - a_0^2}} \arctan \left(\frac{(b - a_0) \tanh[0.5kt] + d}{\sqrt{b^2 - d^2 - a_0^2}} \right) + a_0 \ln \left(\frac{\tanh[0.5kt + 1]}{\tanh[0.5kt - 1]} \right) \right]. \quad (4.54)$$

The corresponding potential is given by

$$V_2 = -\frac{0.5\epsilon\phi_0^2}{(a_0 + b \cosh[kt] + d \sinh[kt])^2} + \frac{k^2}{3} \left(\frac{b \sinh[kt] + d \cosh[kt]}{a_0 + b \cosh[kt] + d \sinh[kt]} \right)^2. \quad (4.55)$$

The energy density and pressure have the forms

$$\rho_4 = \frac{k^2}{3} \left(\frac{b \sinh[kt] + d \cosh[kt]}{a_0 + b \cosh[kt] + d \sinh[kt]} \right)^2, \quad (4.56)$$

$$p_4 = -\frac{k^2}{3} \frac{(b \sinh[kt] + d \cosh[kt])^2 - 2[a_0(b \cosh[kt] + d \sinh[kt]) + b^2 - d^2]}{(a_0 + b \cosh[kt] + d \sinh[kt])^2}. \quad (4.57)$$

For this example, the EoS and the deceleration parameter become

$$\omega_4 = -1 - \frac{2[a_0(b \cosh[kt] + d \sinh[kt]) + b^2 - d^2]}{(b \sinh[kt] + d \cosh[kt])^2} \quad (4.58)$$

and

$$q_4 = -1 - \frac{3[a_0(b \cosh[kt] + d \sinh[kt]) + b^2 - d^2]}{(b \sinh[kt] + d \cosh[kt])^2}, \quad (4.59)$$

respectively.

In Fig. 11, we depict the cosmological evolutions of the energy density ρ_4 and pressure p_4 as functions of t . In Fig. 12, we show the cosmological evolution of the EoS w_4 as a function of t . From Fig. 12, we understand that also in this example the crossing of the phantom

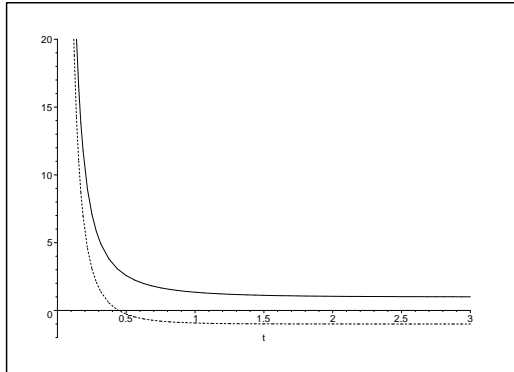


FIG. 11: ρ_4 (solid line) and p_4 (dotted line) as functions of t .

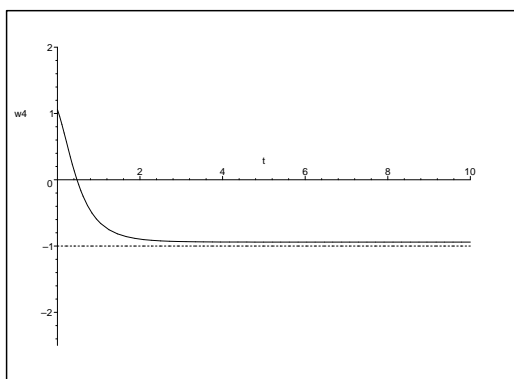


FIG. 12: w_4 as a function of t for $a_0 = -1/2$, $b = 1/2$, $d = 1$ and $k = \sqrt{3}$.

divide cannot be realized. Moreover, the jerk parameter is described by

$$j_4 = \frac{9a_0^2 - 10b^2 + 9d^2 + (b^2 + d^2) \cosh^2[kt] + bd \sinh[2kt]}{(b \sinh[kt] + d \cosh[kt])^2}. \quad (4.60)$$

In Fig. 13, we illustrate the cosmological evolutions of the deceleration parameter q_4 and jerk parameter j_4 as functions of t .

In summary, from Figs. 2, 5, 8 and 12 we see that in the above four models, the universe is always in the non-phantom (quintessence) phase (in which $w > -1$) and therefore the crossing of the phantom divide cannot be realized.

B. Solutions with the crossing of the phantom divide

Next, in this subsection we investigate the solutions in four examples with realizing the crossing of the phantom divide.

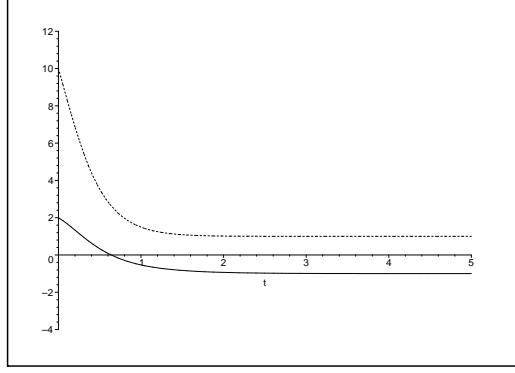


FIG. 13: q_4 (solid line) and j_4 (dotted line) as functions of t .

1. Example 1

We consider that the scale factor is described by

$$a = e^{\frac{2}{3} \int \frac{dt}{t - \int t \tan[\frac{1}{t}] dt}}. \quad (4.61)$$

In this example, we acquire

$$H = \frac{2}{3(t - \int t \tan[\frac{1}{t}] dt)}, \quad (4.62)$$

$$u = c e^{-2 \int \frac{dt}{t - \int t \tan[\frac{1}{t}] dt}}, \quad (4.63)$$

$$\dot{\phi} = \phi_0 e^{-2 \int \frac{dt}{t - \int t \tan[\frac{1}{t}] dt}}, \quad (4.64)$$

$$\psi_l = c_l e^{iD - \int \frac{dt}{t - \int t \tan[\frac{1}{t}] dt}}, \quad (4.65)$$

$$\psi_k = c_k e^{-iD - \int \frac{dt}{t - \int t \tan[\frac{1}{t}] dt}}, \quad (4.66)$$

where

$$D = \frac{1}{c \sigma} \int \left[\frac{4(t \tan[\frac{1}{t}] - 1)}{3(t - \int t \tan[\frac{1}{t}] dt)^2} e^{2 \int \frac{dt}{t - \int t \tan[\frac{1}{t}] dt}} + \phi_0^2 e^{-2 \int \frac{dt}{t - \int t \tan[\frac{1}{t}] dt}} \right] dt. \quad (4.67)$$

The form of the corresponding potential reads

$$V_2 = -0.5 \epsilon \phi_0^2 e^{-4 \int \frac{dt}{t - \int t \tan[\frac{1}{t}] dt}} + \frac{4}{3(t - \int t \tan[\frac{1}{t}] dt)^2}. \quad (4.68)$$

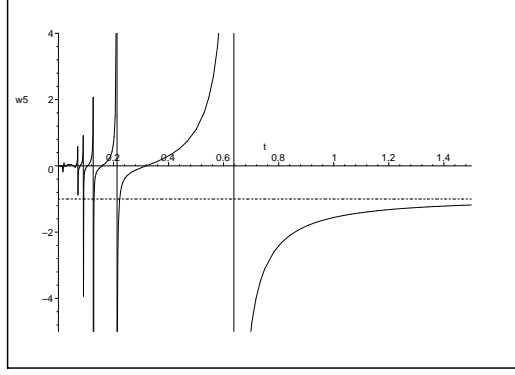


FIG. 14: w_5 as a function of t .

The energy density and pressure are given by

$$\rho_5 = \frac{4}{3(t - \int t \tan[\frac{1}{t}] dt)^2}, \quad p_5 = -\frac{4t \tan[\frac{1}{t}]}{3(t - \int t \tan[\frac{1}{t}] dt)^2}. \quad (4.69)$$

For this example, the EoS and the deceleration parameter are written by

$$w_5 = -t \tan[\frac{1}{t}] \quad (4.70)$$

and

$$q_5 = 0.5 - 1.5t \tan[\frac{1}{t}], \quad (4.71)$$

respectively.

In Fig. 14, we display the EoS w_5 as a function of t . From Fig. 14, we see that in this model the crossing of the phantom divide can be realized. In addition, the jerk parameter is described by

$$j_5 = -\frac{1}{4t} \left[5t + 9t \tan[\frac{1}{t}] \left(t - (2t^2 - 1) \tan[\frac{1}{t}] \right) + 9 \left(t \tan[\frac{1}{t}] - \tan^2[\frac{1}{t}] - 1 \right) \int t \tan[\frac{1}{t}] dt \right]. \quad (4.72)$$

2. Example 2

We take the scale factor as

$$a = e^{\frac{2}{3} \int \frac{dt}{t - 0.5(t^2 \sin[\frac{1}{t}] + t \cos[\frac{1}{t}])}}. \quad (4.73)$$

In this case, we find

$$H = \frac{2}{3[t - 0.5(t^2 \sin[\frac{1}{t}] + t \cos[\frac{1}{t}])]} , \quad (4.74)$$

$$u = c e^{-2 \int \frac{dt}{t - 0.5(t^2 \sin[\frac{1}{t}] + t \cos[\frac{1}{t}])}} , \quad (4.75)$$

$$\dot{\phi} = \phi_0 e^{-2 \int \frac{dt}{t - 0.5(t^2 \sin[\frac{1}{t}] + t \cos[\frac{1}{t}])}} , \quad (4.76)$$

$$\psi_l = c_l e^{iD - \int \frac{dt}{t - 0.5(t^2 \sin[\frac{1}{t}] + t \cos[\frac{1}{t}])}} , \quad (4.77)$$

$$\psi_k = c_k e^{-iD - \int \frac{dt}{t - 0.5(t^2 \sin[\frac{1}{t}] + t \cos[\frac{1}{t}])}} , \quad (4.78)$$

where

$$D = \frac{1}{c \sigma} \int \left[\frac{4(1 - [t + 0.5t^{-1}] \sin[\frac{1}{t}])}{3(t - 0.5(t^2 \sin[\frac{1}{t}] + t \cos[\frac{1}{t}]))^2} e^{2 \int \frac{dt}{t - 0.5(t^2 \sin[\frac{1}{t}] + t \cos[\frac{1}{t}])}} + \phi_0^2 \int e^{-2 \int \frac{dt}{t - 0.5(t^2 \sin[\frac{1}{t}] + t \cos[\frac{1}{t}])}} \right] dt . \quad (4.79)$$

The corresponding potential is given by

$$V_2 = -0.5\epsilon\phi_0^2 e^{-4 \int \frac{dt}{t - 0.5(t^2 \sin[\frac{1}{t}] + t \cos[\frac{1}{t}])}} + \frac{4}{3[t - 0.5(t^2 \sin[\frac{1}{t}] + t \cos[\frac{1}{t}])]^2} . \quad (4.80)$$

The forms of the energy density and pressure become

$$\rho_6 = \frac{4}{3[t - 0.5(t^2 \sin[\frac{1}{t}] + t \cos[\frac{1}{t}])]^2} , \quad p_6 = -\frac{4(t + 0.5t^{-1}) \sin[\frac{1}{t}]}{3[t - 0.5(t^2 \sin[\frac{1}{t}] + t \cos[\frac{1}{t}])]^2} . \quad (4.81)$$

For this example, the EoS and the deceleration parameter are given by

$$w_6 = -(t + 0.5t^{-1}) \sin[\frac{1}{t}] \quad (4.82)$$

and

$$q_6 = 0.5 - 1.5(t + 0.5t^{-1}) \sin[\frac{1}{t}] , \quad (4.83)$$

respectively.

In Fig. 15, we display the cosmological evolution of the energy density ρ_6 and pressure p_6 as functions of t . In Fig. 16, we show the cosmological evolution of the EoS w_6 as a function

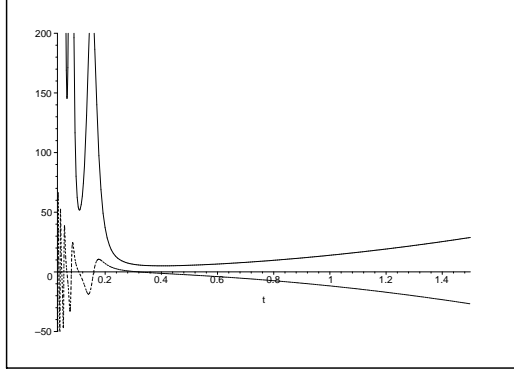


FIG. 15: ρ_6 (solid line) and p_6 (dotted line) as functions of t .

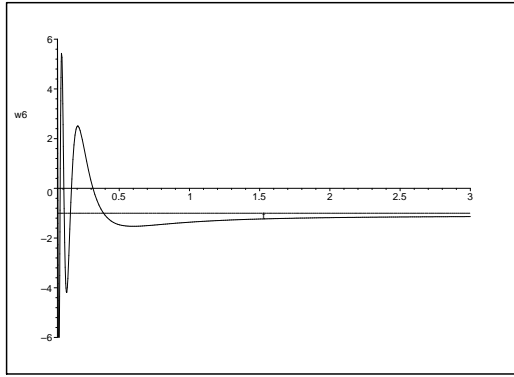


FIG. 16: w_6 as a function of t .

of t . It follows from Fig. 16 that in this case the crossing of the phantom divide can occur. Furthermore, the jerk parameter is expressed as

$$j_6 = \frac{1}{16t^2} [18 + 97t^2 + 9t \sin[\frac{2}{t}] + 18t(3t^3 \sin[\frac{1}{t}] - 2t^2 - 3) \sin[\frac{1}{t}] - 9(\cos[\frac{1}{t}](7t^2 + 1) + 4t^2 + 2) \cos[\frac{1}{t}]]. \quad (4.84)$$

In Fig. 17, we demonstrate the cosmological evolutions of the deceleration parameter q_6 and jerk parameter j_6 as functions of t .

3. Example 3

We express the scale factor as

$$a = a_0 + b \sin[kt] + d \cos[kt], \quad (4.85)$$

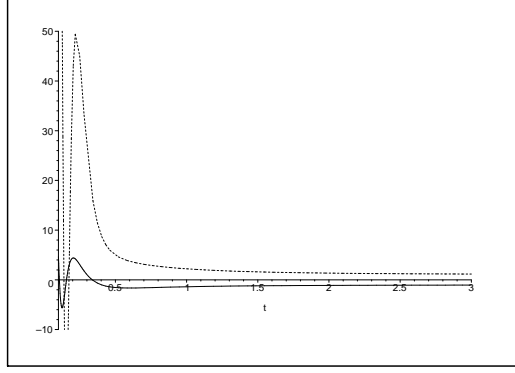


FIG. 17: q_6 (solid line) and j_6 (dotted line) as functions of t

where a_0 , b , d and k are constants. From this description, we obtain

$$H = \frac{k(b \cos[kt] - d \sin[kt])}{a_0 + b \sin[kt] + d \cos[kt]}, \quad (4.86)$$

$$u = \frac{c}{(a_0 + b \sin[kt] + d \cos[kt])^3}, \quad (4.87)$$

$$\dot{\phi} = \frac{\phi_0}{(a_0 + b \sin[kt] + d \cos[kt])^3}, \quad (4.88)$$

$$\psi_l = \frac{c_l}{(a_0 + b \sin[kt] + d \cos[kt])^{1.5}} e^{iD}, \quad (4.89)$$

$$\psi_k = \frac{c_k}{(a_0 + b \sin[kt] + d \cos[kt])^{1.5}} e^{-iD}, \quad (4.90)$$

where

$$D = \frac{1}{c \sigma} \int (2k^2(a_0 + b \sin[kt] + d \cos[kt])(a_0(b \sin[kt] + d \cos[kt]) + b^2 + d^2) + \phi_0^2(a_0 + b \sin[kt] + d \cos[kt])^{-3}) dt. \quad (4.91)$$

The corresponding potential is given by

$$V_2 = -\frac{0.5\epsilon\phi_0^2}{(a_0 + b \sin[kt] + d \cos[kt])^6} + 3k^2 \left(\frac{b \cos[kt] - d \sin[kt]}{a_0 + b \sin[kt] + d \cos[kt]} \right)^2. \quad (4.92)$$

The energy density and the pressure have the forms

$$\rho_7 = 3k^2 \left(\frac{b \cos[kt] - d \sin[kt]}{a_0 + b \sin[kt] + d \cos[kt]} \right)^2, \quad (4.93)$$

$$p_7 = -k^2 \frac{3(b \cos[kt] - d \sin[kt])^2 - 2[a_0(b \sin[kt] + d \cos[kt]) + b^2 + d^2]}{(a_0 + b \sin[kt] + d \cos[kt])^2}. \quad (4.94)$$

In this example, the EoS and the deceleration parameter are described as

$$w_7 = -1 + \frac{2[a_0(b \sin[kt] + d \cos[kt]) + b^2 + d^2]}{3(b \cos[kt] - d \sin[kt])^2} \quad (4.95)$$

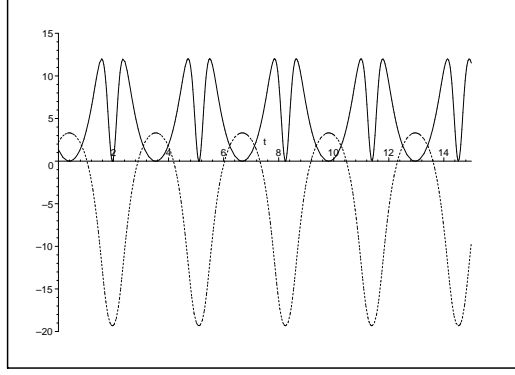


FIG. 18: ρ_7 (solid line) and p_7 (dotted line) as a functions of t for $a_0 = 2$, $b = 1$, $d = 1$ and $k = 2$.

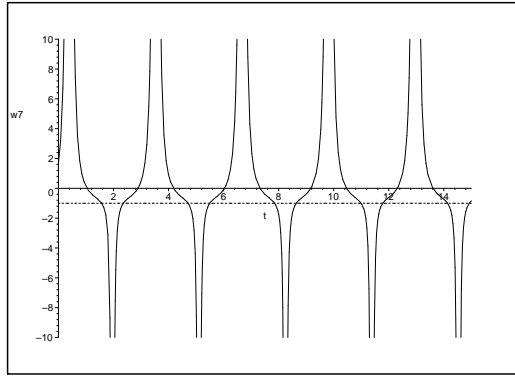


FIG. 19: w_7 as a function of t for $a_0 = 2$, $b = 1$, $d = 1$ and $k = 2$.

and

$$q_7 = -1 + \frac{[a_0(b \sin[kt] + d \cos[kt]) + b^2 + d^2]}{(b \cos[kt] - d \sin[kt])^2}, \quad (4.96)$$

respectively.

In Fig. 18, we show the cosmological evolutions of the energy density ρ_7 and pressure p_7 as the functions of t . In Fig. 19, we illustrate the cosmological evolution of the EoS w_7 as a function of t . We find from Fig. 19 that in this model the crossing of the phantom divide can happen. Furthermore, the jerk parameter is written by

$$j_7 = -\frac{(a_0 + b \sin[kt] + d \cos[kt])^2}{(b^2 - d^2) \cos^2[kt] - bd \sin[2kt] + d^2}. \quad (4.97)$$

In Fig. 20, we display the cosmological evolutions of the deceleration parameter q_7 and jerk parameter j_7 as functions of t .

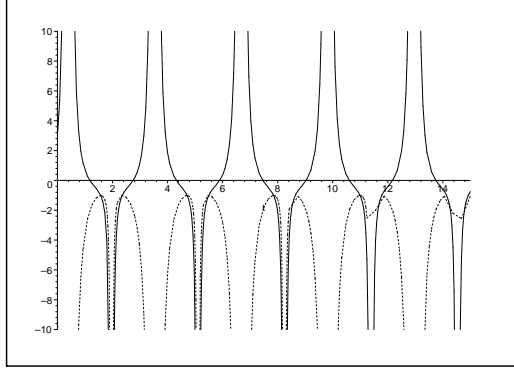


FIG. 20: q_2 (solid line) and j_2 (dotted line) as functions of t .

4. Example 4

We start from the following expression for the scale factor

$$a = e^{\frac{2}{3} \int \frac{dt}{t + \int (lf^{-2} + mf^{-1} + n) dt}}, \quad (4.98)$$

where $f = a_0 + b \cosh[kt] + d \sinh[kt]$, and l, m, n, a_0, b, d and k are constants. Then, we obtain

$$H = \frac{2}{3[t + \int (lf^{-2} + mf^{-1} + n) dt]}, \quad (4.99)$$

$$u = c e^{-2 \int \frac{dt}{t + \int (lf^{-2} + mf^{-1} + n) dt}}, \quad (4.100)$$

$$\dot{\phi} = \phi_0 e^{-2 \int \frac{dt}{t + \int (lf^{-2} + mf^{-1} + n) dt}}, \quad (4.101)$$

$$\psi_l = c_l e^{iD - \int \frac{dt}{t + \int (lf^{-2} + mf^{-1} + n) dt}}, \quad (4.102)$$

$$\psi_k = c_k e^{-iD - \int \frac{dt}{t + \int (lf^{-2} + mf^{-1} + n) dt}}, \quad (4.103)$$

where

$$D = \frac{1}{c \sigma} \int \left(-\frac{4(1 + lf^{-2} + mf^{-1} + n)}{3(t + \int (lf^{-2} + mf^{-1} + n) dt)^2} e^{2 \int \frac{dt}{t + \int (lf^{-2} + mf^{-1} + n) dt}} + \phi_0^2 \int e^{-2 \int \frac{dt}{t + \int (lf^{-2} + mf^{-1} + n) dt}} \right) dt. \quad (4.104)$$

The corresponding potential becomes

$$V_2 = -0.5\epsilon\phi_0^2 e^{-4f \frac{dt}{t + \int (lf^{-2} + mf^{-1} + n)dt}} + \frac{4}{3[t + \int (lf^{-2} + mf^{-1} + n)dt]^2}. \quad (4.105)$$

The energy density and pressure are given by

$$\rho_8 = \frac{4}{3[t + \int (lf^{-2} + mf^{-1} + n)dt]^2}, \quad (4.106)$$

$$p_8 = -\frac{4(lf^{-2} + mf^{-1} + n)}{3[t + \int (lf^{-2} + mf^{-1} + n)dt]^2}. \quad (4.107)$$

In this example, the EoS and the deceleration parameter have the following forms

$$w_8 = lf^{-2} + mf^{-1} + n \quad (4.108)$$

and

$$q_8 = 0.5 + 1.5(lf^{-2} + mf^{-1} + n), \quad (4.109)$$

or

$$w_8 = l(a_0 + b \cosh[kt] + d \sinh[kt])^{-2} + m(a_0 + b \cosh[kt] + d \sinh[kt])^{-1} + n \quad (4.110)$$

and

$$q_8 = 0.5 + 1.5(l(a_0 + b \cosh[kt] + d \sinh[kt])^{-2} + m(a_0 + b \cosh[kt] + d \sinh[kt])^{-1} + n). \quad (4.111)$$

In Fig. 21, we illustrate the EoS w_8 as a function of t . From Fig. 21, we understand that in this case the crossing of the phantom divide can be realized from the non-phantom (quintessence) phase (in which $w > -1$) to the phantom one (in which $w < -1$). Moreover, the jerk parameter is described by

$$j_8 = \frac{1}{4f^4} [18(f^2l + f^3m + l^2) + 36lf(m + n) + 18mf^2(m + 2fn) + 2f^4(2 + 9n^2) + 9f\dot{f}(2l + fm)[t + \int (lf^{-2} + mf^{-1} + n)dt]]. \quad (4.112)$$

As a consequence, from Figs. 2, 5, 8 and 12 we understand that in the above four models, the universe is always in the non-phantom (quintessence) phase and therefore the crossing of the phantom divide cannot be realized. In particular, in the first three examples, the phantom crossing from the non-phantom phase to the phantom one and that from the phantom phase to the non-phantom one can occur. Moreover, in the last example, the

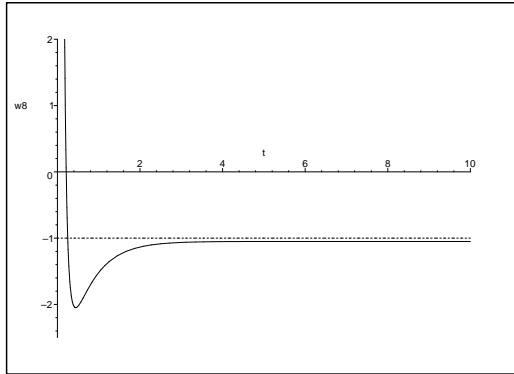


FIG. 21: w_8 as a function of t for $l = 1$, $m = -2$, $n = -1$, $a_0 = -1/2$, $b = 1/2$, $d = 1$ and $k = \sqrt{3}$.

crossing of the phantom divide can be realized from the non-phantom (quintessence) phase to the phantom one (in which $w < -1$). Such a transition behavior is consistent with the observational suggestions [46–51]. We also note that the qualitative behaviors of the numerical results shown in Figs. 1–21 do not strongly depend on the initial conditions as well as the model parameters. Presumably, from such a nature it seems that even if we include matter, the matter-dominated stage would be realized and an attractor solution could be realized.

We caution that the solutions reconstructed in this work might well be unstable. In addition, there appears divergence in the effective energy density in most of the examples during finite time. The stability of those models will be a crucial problem, which will spoil the models even if matter sectors are included. Accordingly, in order to solve this stability issue, we have to extend the present toy models to be more elaborate ones. Indeed, the resultant solutions could correspond to more complex models such as theories with non-linear kinetic terms, e.g., the ghost condensate scenario [79] and the Galileon gravity models [80–84]. It would be the most important future work of the present paper to examine the stability of the obtained solutions by comparing with the above theories which consist of non-linear kinetic terms, so that we can find some clue for the mechanism to make the derived cosmological solutions viable.

Consequently, the divergence or oscillating behavior of effective energy density will dramatically change the history of the universe, so that the process of the nucleosynthesis will probably be spoiled. Thus, it is crucial task for the present models to preserve the big bang nucleosynthesis (BBN), so that g-essence models can be realistic ones which are able to successfully resolve the mechanism of the current accelerated expansion of the universe.

Furthermore, we also note that the reconstructed expression of the potential V_2 is given by a function of t and that of not ϕ . This is because it is difficult to obtain the explicit analytic form of $V_2 = V_2(\bar{\psi}\psi)$ and we find the analytic representation of $\dot{\phi}$ and that of not ϕ . In this respect, the reconstructed procedure performed in this work would not be perfect in order to derive the form of a g-essence model as a scalar field theory and investigate the effective mass through the potential expression. Since we concentrate on the cosmological evolution of the EoS for dark energy, the reconstruction of explicit form of the potential is an additional result of this work. In fact, it should be noted that what $V_2(\bar{\psi}\psi)$ is given as a solution of the equations of motion is very peculiar. In this work, we consider a toy model of g-essence in terms of the fermion ψ phenomenologically. However, if we take a concrete fundamental theory in particle physics, it is considered that the particle physics theory can present the form of such kind of effective potential for ψ . Furthermore, this situation would be similar to that in the quintessence models on the level that the potential cannot be given by particle physics because we do not have any particle physics theory which can give the very small mass of quintessence to realize the current cosmic acceleration, namely, in order for the current value of the quintessence potential to be equal to the very small value of the cosmological constant at the present universe.

Finally, it is meaningful to emphasize the novel ingredients of this work. In g-essence models, there exist two dynamical components. One is the scalar field ϕ . Another is the fermion condensate $u = \bar{\psi}\psi$. These two components play a role of dark energy. In our analysis, the dynamics of both ϕ and u is included. As a consequence, the evolutions of cosmological quantities such as the deceleration parameter, the jerk parameter and the EoS in g-essence models become different from those in two scalar field models. This is one of the most important results obtained in this work. In addition, in Sec. IV B we explicitly illustrate that there exist g-essence models in which the crossing of the phantom divide can be realized. In general, from the quantum field theoretical view, in a single scalar field theory, if the EoS of the scalar field is less than -1 , i.e., the universe is in the phantom phase, then the null energy condition is violated, so that the vacuum can be unstable, and hence there will appear microphysical ghosts. However, in g-essence models, in the field equation level there exist couplings of the fermion fields to H , and thus the dynamics of all the fields in the basic system is not exactly equivalent to that in a single scalar field theory. Accordingly, it is not so trivial whether the ghosts will exist in g-essence models examined

in Sec. IV B and the vacuum will be unstable. The investigations on the existence of the ghosts as well as the instabilities of the vacuum such as Laplace instabilities should be the future work in our studies of g-essence models with realizing the crossing of the phantom divide. The main purpose of this paper is to illustrate that the crossing of the phantom divide can occur in the framework of g-essence models, although there have been proposed other simpler models showing the crossing of the phantom divide in the literature.

V. CONCLUSIONS

In the present paper, we have studied the cosmological EoS for dark energy in g-essence models. In particular, we have found several g-essence models in which the universe is always in the non-phantom (quintessence) phase and thus the crossing of the phantom divide cannot occur. Furthermore, we have examined an explicit g-essence model in which the crossing of the phantom divide can be realized from the non-phantom phase to the phantom one. This transition manner is compatible with the analyses of the recent various cosmological observational data [46–51].

We remark that in Ref. [6], the limit on a constant EoS for dark energy has been analyzed as $w_{\text{DE}} = -1.10 \pm 0.14$ (68% CL) in a flat universe. Moreover, in case of a time-dependent EoS for dark energy obeying a linear form $w_{\text{DE}}(a) = w_{\text{DE}0} + w_{\text{DE}a}(1 - a)$ [85, 86] with $w_{\text{DE}0}$ and $w_{\text{DE}a}$ being the current value of w_{DE} and its derivative, respectively, the constraints have been estimated as $w_{\text{DE}0} = -0.93 \pm 0.13$ and $w_{\text{DE}a} = -0.41^{+0.72}_{-0.71}$ (68% CL) [6]. If the more precise future CMB experiments such as PLANCK [87] support the phantom phase, the studies on the crossing of the phantom divide become more important in order to investigate the nature and property of dark energy. Thus, it can be considered that our results would be worthy of a clue to obtain the significant features of dark energy.

Acknowledgments

K.B. would like to sincerely appreciate very kind and warm hospitality at Eurasian National University very much, where this work has been executed.

-
- [1] S. Perlmutter *et al.* [SNCP Collaboration], *Astrophys. J.* **517**, 565 (1999) [arXiv:astro-ph/9812133].
 - [2] A. G. Riess *et al.* [Supernova Search Team Collaboration], *Astron. J.* **116**, 1009 (1998) [arXiv:astro-ph/9805201].
 - [3] D. N. Spergel *et al.* [WMAP Collaboration], *Astrophys. J. Suppl.* **148**, 175 (2003) [arXiv:astro-ph/0302209].
 - [4] D. N. Spergel *et al.* [WMAP Collaboration], *Astrophys. J. Suppl.* **170**, 377 (2007) [arXiv:astro-ph/0603449].
 - [5] E. Komatsu *et al.* [WMAP Collaboration], *Astrophys. J. Suppl.* **180**, 330 (2009) [arXiv:0803.0547 [astro-ph]].
 - [6] E. Komatsu *et al.* [WMAP Collaboration], *Astrophys. J. Suppl.* **192**, 18 (2011) [arXiv:1001.4538 [astro-ph.CO]].
 - [7] G. Hinshaw, D. Larson, E. Komatsu, D. N. Spergel, C. L. Bennett, J. Dunkley, M. R.olta and M. Halpern *et al.*, arXiv:1212.5226 [astro-ph.CO].
 - [8] M. Tegmark *et al.* [SDSS Collaboration], *Phys. Rev. D* **69**, 103501 (2004) [arXiv:astro-ph/0310723].
 - [9] U. Seljak *et al.* [SDSS Collaboration], *Phys. Rev. D* **71**, 103515 (2005) [arXiv:astro-ph/0407372].
 - [10] D. J. Eisenstein *et al.* [SDSS Collaboration], *Astrophys. J.* **633**, 560 (2005) [arXiv:astro-ph/0501171].
 - [11] B. Jain and A. Taylor, *Phys. Rev. Lett.* **91**, 141302 (2003) [arXiv:astro-ph/0306046].
 - [12] P. J. E. Peebles and B. Ratra, *Astrophys. J.* **325**, L17 (1988).
 - [13] B. Ratra and P. J. E. Peebles, *Phys. Rev. D* **37**, 3406 (1988).
 - [14] T. Chiba, N. Sugiyama and T. Nakamura, *Mon. Not. Roy. Astron. Soc.* **289**, L5 (1997) [arXiv:astro-ph/9704199].

- [15] R. R. Caldwell, R. Dave and P. J. Steinhardt, Phys. Rev. Lett. **80**, 1582 (1998) [arXiv:astro-ph/9708069].
- [16] I. Zlatev, L. M. Wang and P. J. Steinhardt, Phys. Rev. Lett. **82**, 896 (1999) [arXiv:astro-ph/9807002].
- [17] T. Chiba, T. Okabe and M. Yamaguchi, Phys. Rev. D **62**, 023511 (2000) [arXiv:astro-ph/9912463].
- [18] C. Armendariz-Picon, T. Damour and V. F. Mukhanov, Phys. Lett. B **458**, 209 (1999) [arXiv:hep-th/9904075].
- [19] J. Garriga and V. F. Mukhanov, Phys. Lett. B **458**, 219 (1999) [arXiv:hep-th/9904176].
- [20] C. Armendariz-Picon, V. F. Mukhanov and P. J. Steinhardt, Phys. Rev. Lett. **85**, 4438 (2000) [arXiv:astro-ph/0004134].
- [21] C. Armendariz-Picon, V. F. Mukhanov and P. J. Steinhardt, Phys. Rev. D **63**, 103510 (2001) [arXiv:astro-ph/0006373].
- [22] R. de Putter and E. V. Linder, Astropart. Phys. **28**, 263 (2007) [arXiv:0705.0400 [astro-ph]].
- [23] A. Y. Kamenshchik, U. Moschella and V. Pasquier, Phys. Lett. B **511**, 265 (2001) [arXiv:gr-qc/0103004].
- [24] M. C. Bento, O. Bertolami and A. A. Sen, Phys. Rev. D **66** (2002) 043507 [arXiv:gr-qc/0202064].
- [25] E. J. Copeland, M. Sami and S. Tsujikawa, Int. J. Mod. Phys. D **15**, 1753 (2006) [arXiv:hep-th/0603057].
- [26] R. Durrer and R. Maartens, Gen. Rel. Grav. **40**, 301 (2008) [arXiv:0711.0077 [astro-ph]].
- [27] R. Durrer and R. Maartens, arXiv:0811.4132 [astro-ph].
- [28] Y. F. Cai, E. N. Saridakis, M. R. Setare and J. Q. Xia, Phys. Rept. **493**, 1 (2010) [arXiv:0909.2776 [hep-th]].
- [29] S. Tsujikawa, arXiv:1004.1493 [astro-ph.CO].
- [30] L. Amendola and S. Tsujikawa, *Dark Energy* (Cambridge University press, 2010).
- [31] M. Li, X. D. Li, S. Wang and Y. Wang, Commun. Theor. Phys. **56**, 525 (2011) [arXiv:1103.5870 [astro-ph.CO]].
- [32] K. Bamba, S. Capozziello, S. Nojiri and S. D. Odintsov, Astrophys. Space Sci. **342**, 155 (2012) [arXiv:1205.3421 [gr-qc]].
- [33] K. R. Yesmakhanova, N. A. Myrzakulov, K. K. Yerzhanov, G. N. Nugmanova, N. S. Serik-

- bayaev and R. Myrzakulov, arXiv:1201.4360 [physics.gen-ph].
- [34] A. J. Lopez-Revelles, R. Myrzakulov and D. Saez-Gomez, Phys. Rev. D **85**, 103521 (2012) [arXiv:1201.5647 [gr-qc]].
- [35] K. Bamba, K. Yesmakhanova, K. Yerzhanov and R. Myrzakulov, arXiv:1203.3401 [gr-qc].
- [36] K. Bamba, U. Debnath, K. Yesmakhanova, P. Tsyba, G. Nugmanova and R. Myrzakulov, Entropy **14**, 2351 (2012) [arXiv:1203.4226 [gr-qc]].
- [37] R. Myrzakulov arXiv:1204.1093 [physics.gen-ph].
- [38] S. Nojiri and S. D. Odintsov, Phys. Rept. **505**, 59 (2011) [arXiv:1011.0544 [gr-qc]].
- [39] S. Nojiri and S. D. Odintsov, eConf **C0602061**, 06 (2006) [Int. J. Geom. Meth. Mod. Phys. **4**, 115 (2007)] [arXiv:hep-th/0601213].
- [40] T. P. Sotiriou and V. Faraoni, Rev. Mod. Phys. **82**, 451 (2010) [arXiv:0805.1726 [gr-qc]].
- [41] S. Capozziello and V. Faraoni, *Beyond Einstein Gravity* (Springer, 2010).
- [42] S. Capozziello and M. De Laurentis, Phys. Rept. **509**, 167 (2011) [arXiv:1108.6266 [gr-qc]].
- [43] A. De Felice and S. Tsujikawa, Living Rev. Rel. **13**, 3 (2010) [arXiv:1002.4928 [gr-qc]].
- [44] T. Clifton, P. G. Ferreira, A. Padilla and C. Skordis, Phys. Rept. **513**, 1 (2012) [arXiv:1106.2476 [astro-ph.CO]].
- [45] S. Capozziello, M. De Laurentis and S. D. Odintsov, Eur. Phys. J. C **72**, 2068 (2012) [arXiv:1206.4842 [gr-qc]].
- [46] U. Alam, V. Sahni, T. D. Saini and A. A. Starobinsky, Mon. Not. Roy. Astron. Soc. **354**, 275 (2004) [astro-ph/0311364].
- [47] U. Alam, V. Sahni and A. A. Starobinsky, JCAP **0406**, 008 (2004) [arXiv:astro-ph/0403687].
- [48] U. Alam, V. Sahni and A. A. Starobinsky, JCAP **0702**, 011 (2007) [arXiv:astro-ph/0612381].
- [49] S. Nesseris and L. Perivolaropoulos, JCAP **0701**, 018 (2007) [arXiv:astro-ph/0610092].
- [50] P. U. Wu and H. W. Yu, Phys. Lett. B **643**, 315 (2006) [arXiv:astro-ph/0611507].
- [51] H. K. Jassal, J. S. Bagla and T. Padmanabhan, Mon. Not. Roy. Astron. Soc. **405**, 2639 (2010) [arXiv:astro-ph/0601389].
- [52] R. Myrzakulov, arXiv:1011.4337 [astro-ph.CO].
- [53] K. Bamba, C. Q. Geng and C. C. Lee, JCAP **1008**, 021 (2010) [arXiv:1005.4574 [astro-ph.CO]].
- [54] E. V. Linder, Phys. Rev. D **81**, 127301 (2010) [Erratum-ibid. D **82**, 109902 (2010)] [arXiv:1005.3039 [astro-ph.CO]].
- [55] K. Bamba, C. Q. Geng, C. C. Lee and L. W. Luo, JCAP **1101**, 021 (2011) [arXiv:1011.0508

- [astro-ph.CO]].
- [56] K. Bamba, C. Q. Geng and C. C. Lee, arXiv:1008.4036 [astro-ph.CO].
- [57] K. Bamba, R. Myrzakulov, S. Nojiri and S. D. Odintsov, Phys. Rev. D **85**, 104036 (2012) [arXiv:1202.4057 [gr-qc]].
- [58] M. Jamil, D. Momeni and R. Myrzakulov, Eur. Phys. J. C **72**, 1959 (2012) [arXiv:1202.4926 [physics.gen-ph]].
- [59] R. Myrzakulov, arXiv:1205.5266 [physics.gen-ph].
- [60] A. A. Starobinsky, JETP Lett. **68**, 757 (1998) [Pisma Zh. Eksp. Teor. Fiz. **68**, 721 (1998)] [arXiv:astro-ph/9810431].
- [61] D. Huterer and M. S. Turner, Phys. Rev. D **60**, 081301 (1999) [arXiv:astro-ph/9808133].
- [62] T. Nakamura and T. Chiba, Mon. Not. Roy. Astron. Soc. **306**, 696 (1999) [arXiv:astro-ph/9810447].
- [63] V. Sahni and A. Starobinsky, Int. J. Mod. Phys. D **15**, 2105 (2006) [arXiv:astro-ph/0610026].
- [64] S. Nojiri and S. D. Odintsov, Phys. Rev. D **74** (2006) 086005 [arXiv:hep-th/0608008].
- [65] S. Nojiri and S. D. Odintsov, J. Phys. Conf. Ser. **66** (2007) 012005 [arXiv:hep-th/0611071].
- [66] S. Nojiri and S. D. Odintsov, Phys. Rev. D **78**, 046006 (2008) [arXiv:0804.3519 [hep-th]].
- [67] K. Bamba, S. Nojiri and S. D. Odintsov, JCAP **0810**, 045 (2008) [arXiv:0807.2575 [hep-th]].
- [68] S. Nojiri, S. D. Odintsov and D. Saez-Gomez, Phys. Lett. B **681**, 74 (2009) [arXiv:0908.1269 [hep-th]].
- [69] S. Nojiri, S. D. Odintsov and D. Saez-Gomez, AIP Conf. Proc. **1458**, 207 (2011) [arXiv:1108.0767 [hep-th]].
- [70] C. Armendariz-Picon and P. B. Greene, Gen. Rel. Grav. **35**, 1637 (2003) [arXiv:hep-th/0301129].
- [71] O. Razina, P. Tsyba, I. Kulnazarov, S. Myrzakul, K. Yerzhanov and R. Myrzakulov, Eur. Phys. J. Plus **126**, 85 (2011) [arXiv:1101.0729 [astro-ph.CO]].
- [72] O. Razina, Y. Myrzakulov, N. Serikbayev, G. Nugmanova and R. Myrzakulov, Central Eur. J. Phys. **10**, 47 (2012) [arXiv:1012.5690 [astro-ph.CO]].
- [73] I. Kulnazarov, K. Yerzhanov, O. Razina, S. Myrzakul, P. Tsyba and R. Myrzakulov, Eur. Phys. J. C **71**, 1698 (2011) [arXiv:1012.4669 [astro-ph.CO]].
- [74] K. K. Yerzhanov, P. Y. Tsyba, S. R. Myrzakul, I. I. Kulnazarov and R. Myrzakulov, arXiv:1012.3031 [astro-ph.CO].

- [75] M. Sharif, K. Yesmakhanova, S. Rani and R. Myrzakulov, *Eur. Phys. J. C* **72**, 2067 (2012) [arXiv:1204.2181 [physics.gen-ph]].
- [76] T. Damour and C. Hillmann, *JHEP* **0908**, 100 (2009) [arXiv:0906.3116 [hep-th]].
- [77] T. Damour and P. Spindel, *Phys. Rev. D* **83**, 123520 (2011) [arXiv:1103.2927 [gr-qc]].
- [78] V. Sahni, T. D. Saini, A. A. Starobinsky and U. Alam, *JETP Lett.* **77**, 201 (2003) [*Pisma Zh. Eksp. Teor. Fiz.* **77**, 249 (2003)] [arXiv:astro-ph/0201498].
- [79] N. Arkani-Hamed, H. -C. Cheng, M. A. Luty and S. Mukohyama, *JHEP* **0405**, 074 (2004) [hep-th/0312099].
- [80] A. Nicolis, R. Rattazzi and E. Trincherini, *Phys. Rev. D* **79**, 064036 (2009) [arXiv:0811.2197 [hep-th]].
- [81] C. Deffayet, G. Esposito-Farese and A. Vikman, *Phys. Rev. D* **79**, 084003 (2009) [arXiv:0901.1314 [hep-th]].
- [82] C. Deffayet, S. Deser and G. Esposito-Farese, *Phys. Rev. D* **80**, 064015 (2009) [arXiv:0906.1967 [gr-qc]].
- [83] C. Deffayet, S. Deser and G. Esposito-Farese, *Phys. Rev. D* **82**, 061501 (2010) [arXiv:1007.5278 [gr-qc]].
- [84] N. Shirai, K. Bamba, S. Kumekawa, J. Matsumoto and S. Nojiri, *Phys. Rev. D* **86**, 043006 (2012) [arXiv:1203.4962 [hep-th]].
- [85] M. Chevallier and D. Polarski, *Int. J. Mod. Phys. D* **10**, 213 (2001) [arXiv:gr-qc/0009008].
- [86] E. V. Linder, *Phys. Rev. Lett.* **90**, 091301 (2003) [arXiv:astro-ph/0208512].
- [87] <http://www.sciops.esa.int/index.php?project=PLANCK>.